

Ferromagnetic transition in MnP studied by high-resolution photoemission spectroscopy

J. Okabayashi,* K. Tanaka, M. Hashimoto, and A. Fujimori
Department of Physics, The University of Tokyo, Bunkyo-ku, Tokyo 113-0033, Japan

K. Ono
Institute of Materials Structure Science, KEK, Tsukuba, Ibaraki 305-0801, Japan

M. Okusawa
Department of Physics, Faculty of Education, Gunma University, Maebashi, Gunma 371-8510, Japan

T. Komatsubara
Department of Physics, Faculty of Science, Tohoku University, Sendai, Miyagi 980-8578, Japan
 (Received 7 January 2004; published 19 April 2004)

High-resolution photoemission spectroscopy and band-structure calculation were performed on the itinerant ferromagnet MnP. The entire valence-band photoemission spectra and their changes across the Curie temperature were qualitatively described by the band-structure calculation. However, temperature-dependent studies revealed unusual changes such as spectral weight transfer within 2 eV of the Fermi level and the opening of a pseudogap of ~ 100 meV.

DOI: 10.1103/PhysRevB.69.132411

PACS number(s): 75.10.Lp, 71.20.Be, 79.60.-i

The metallic compound MnP exhibits ferromagnetic ordering below the Curie temperature, $T_C=293$ K.¹ Furthermore, below the Neel temperature $T_N=47$ K it transforms into a screw antiferromagnetic (helimagnetic) state.^{2,3} The helical spin structure has been reported to have been ~ 9 periodicity of the lattice spacings along the a axis.⁴ The complex magnetic phase diagram of MnP has attracted considerable interest for many decades. In particular, the Lifshitz point, which is a multicritical point where the ferromagnetic phase, the helimagnetic phase and, the spin-disordered phase meet, has been extensively studied.⁵⁻⁷ From the view point of the electronic structure, it has been controversial whether the Mn $3d$ states are localized or itinerant.^{8,9} A neutron-diffraction study and subsequent analysis have indicated that the screw antiferromagnetic phase is caused by a slight change of the ratio of J_1/J_2 in the Heisenberg model, where J_1 and J_2 are the effective interplanar exchange interaction and next-nearest-neighbor one along the a axis, respectively.^{10,11} The itinerant aspect has been emphasized by photoemission spectroscopy¹² and band-structure calculation.¹³ In fact, MnP is considered as the most itinerant system among the manganese pnictides MnX ($X=P, As, Sb,$ and Bi), where the T_C of MnP is lower than that of MnAs ($T_C=320$ K) (Ref. 14) and MnSb ($T_C=587$ K).¹⁵ As for the electronic structure near the Fermi level (E_F), the Mn $3d$ states have been found dominant in the previous photoemission study⁸ and the specific-heat measurements.¹⁶ Band-structure calculation using the self-consistent augmented-plane-wave method has revealed a large magnetic moment on the Mn atom, the predominance of Mn $3d$ character around E_F , and the importance of $sp-d$ hybridization and resulting $p-d$ exchange interaction for the ferromagnetic ordering.⁹

In order to investigate the electronic structure of itinerant ferromagnetic materials, spin-resolved photoemission spectroscopy has been utilized.¹⁷⁻¹⁹ In the case of Ni metal, the

exchange splitting follows the Stoner model, according to which the splitting disappears above T_C .¹⁷ In the spin-resolved valence-band photoemission study of Fe metal, on the other hand, the exchange splitting persists above T_C ,²⁰ which is theoretically explained by the fluctuation local moment model.²¹ Recently, high-resolution photoemission spectroscopy has opened up new opportunities to investigate the magnetic transition from the view point of the electronic structure. In particular, temperature-dependent high-resolution photoemission spectroscopy is expected to provide us with detailed information related to the temperature dependence of the magnetic properties including the exchange splitting.^{22,23} In this paper, we report on the temperature-dependent high-resolution photoemission study of MnP to investigate changes in the electronic structure associated with the ferromagnetic ordering.

A single crystal of MnP was grown by the Bridgman method. Details of the crystal growth were described elsewhere.²⁴ High-resolution photoemission measurements were performed in the temperature range from 7 K to 320 K using a GAMMADATA-SCIENATA SES-100 photoelectron spectrometer and a high-flux discharging lamp with a toroidal grating monochromator. The base pressure in the spectrometer was 2×10^{-11} Torr and the energy resolution was set at 7 meV and 35 meV for the He I (21.218 eV) and He II (40.814 eV) light sources, respectively. In order to obtain a clean surface, the sample was scraped *in situ* with a diamond file just before each measurement. The Fermi edge of gold evaporated on the sample surface after the measurements was used to determine the E_F position and the instrumental resolution.

We also performed band-structure calculation using a density-functional-theory (DFT)-based pseudopotential package CASTEP (Cambridge serial total energy package),²⁵ where a plane-wave basis set is used for expanding the wave functions and ultrasoft pseudopotentials are used to treat ef-

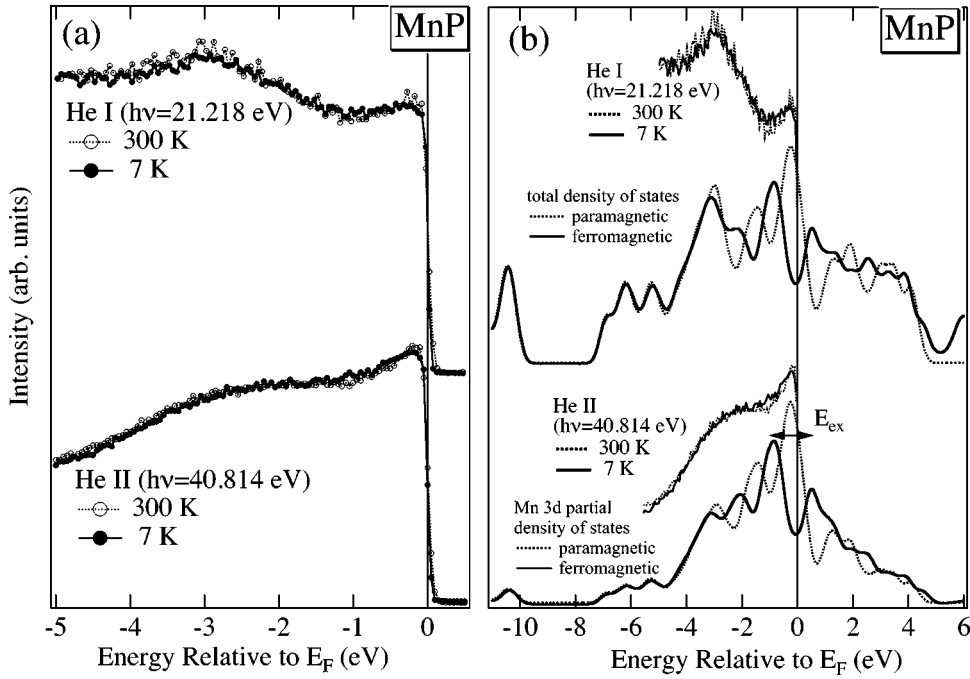


FIG. 1. Photoemission spectra of MnP taken with He I and He II excitations at 300 K (paramagnetic) and 7 K (ferromagnetic). (a) Entire valence band. (b) Band-structure calculation for the paramagnetic and ferromagnetic states and comparison with photoemission spectra. The upper and lower panels show the total density of states and the Mn 3d partial density of states, respectively.

fectively the chemically inactive core electrons. Generalized gradient approximation (GGA) calculations were done for the paramagnetic (nonmagnetic) and ferromagnetic states.

Figure 1(a) shows the entire valence-band spectra taken with He I and He II radiation at 7 K and 300 K. The spectral intensities have been normalized to the area in the energy range from 0.5 eV to -5.0 eV. The overall spectra shown in Fig. 1(a) are in good agreement with the previous reports.^{8,12}

The spectra have a clear Fermi edge indicating the metallic nature of MnP, consistent with the temperature dependence of the resistivity in MnP.²⁶ Results of the DFT-GGA calculations, that is, the total density of states (DOS) and the Mn 3d DOS for the paramagnetic and ferromagnetic states are also shown in Fig. 1(b). The calculated Mn 3d DOS is prominent around E_F and located within ± 4 eV from E_F . The rise of the intensity toward E_F in the He II photoemis-

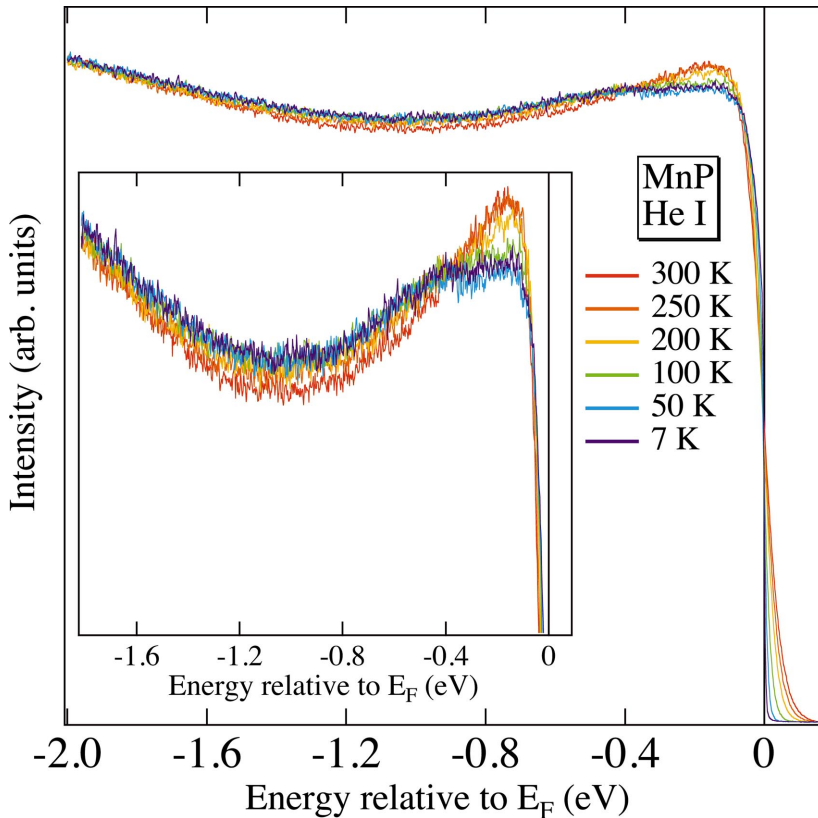


FIG. 2. (Color) Photoemission spectra of MnP taken at various temperatures with He I excitation. Inset shows the expanded plot.

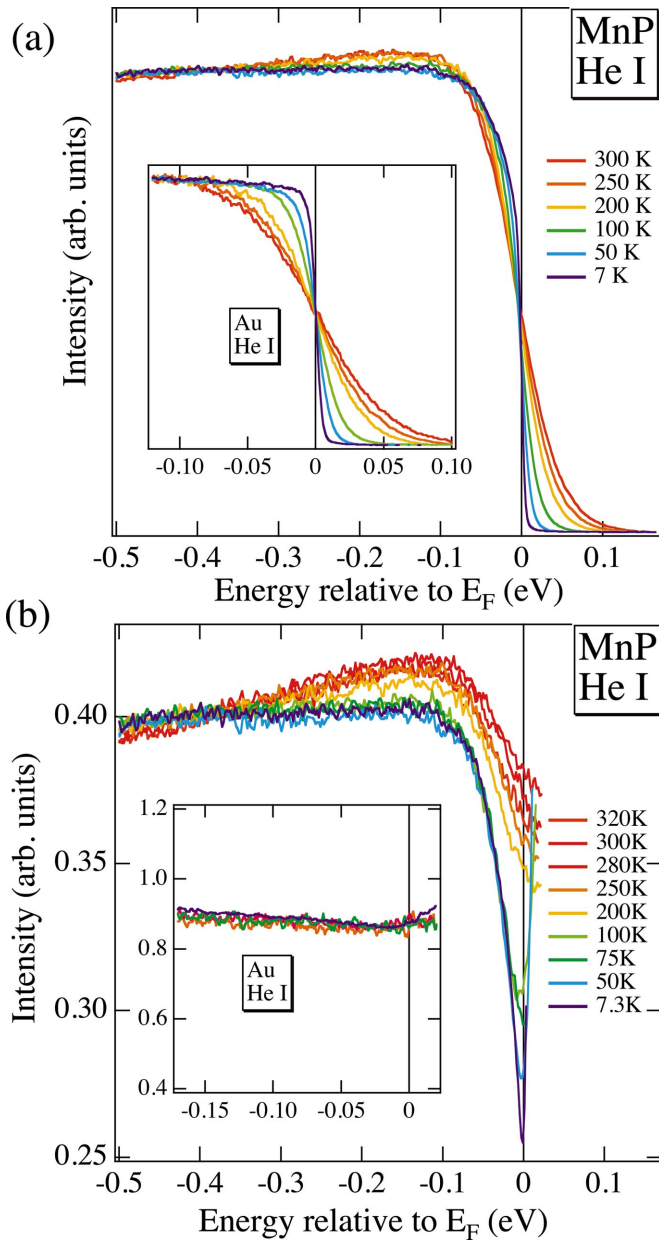


FIG. 3. (Color) Photoemission spectra of MnP taken at various temperatures with He I excitation. (a) Raw data. (b) Spectral DOS obtained by dividing the raw data by the Fermi-Dirac distribution function convoluted with a Gaussian function. Insets show corresponding curves for gold.

sion spectra corresponds to the increase in the calculated Mn $3d$ DOS toward E_F since the photoionization cross section of Mn $3d$ orbitals is enhanced for He II compared to He I.²⁷ In the ferromagnetic state, the calculated peak at E_F is split into two peaks by the exchange splitting. Experimentally the intensity of the Mn $3d$ -derived peak located at E_F decreases with decreasing temperature and the spectral intensity at -1 eV increases with decreasing temperature. This suggests that the photoemission spectra are qualitatively well reproduced by the band-structure calculation including the temperature dependence on this energy scale, meaning that MnP can be considered as an itinerant-electron ferromagnet. Our

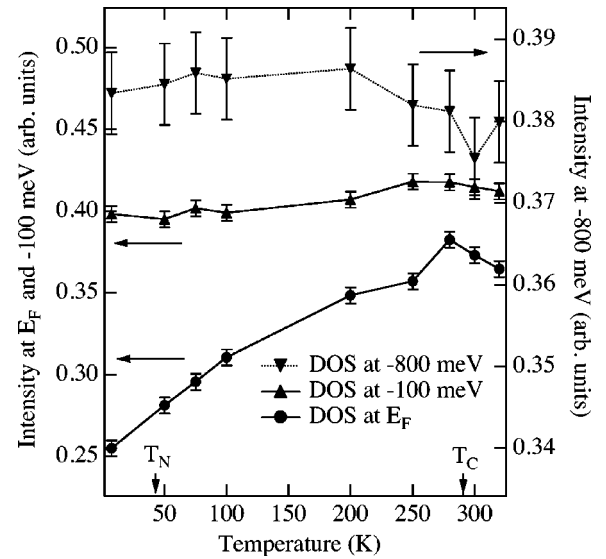


FIG. 4. Temperature-dependent spectral DOS at E_F , -100 meV and -800 meV.

calculation yields the 1.5 eV splitting in the ferromagnetic state resulting in the spin magnetic moments of $3.2 \mu_B/\text{f.u.}$, while the value of the exchange splitting including the effective on-site Coulomb energy (U_{eff}) has been estimated to be 2.2 ± 0.2 eV from the combined photoemission and inverse photoemission spectra.¹² Compared with the band-structure calculations of MnAs and MnSb,¹³ the value of the exchange splitting in MnP is small corresponding to the fact that T_C is lower than those for MnAs and MnSb. The broad structure at -3 eV is due to the P $3p$ states since the intensity increases for He I due to the large cross section of the P $3p$ orbital at lower photon energies.²⁷

In spite of the overall agreement between experiment and calculation, the detailed temperature-dependent studies with higher resolution reveal discrepancy from the band-structure calculation as described below. Figures 2 and 3(a) show the detailed temperature dependence of the photoemission spectra in narrow ranges near E_F measured with He I photons. The spectral intensity in Figs. 2 and 3(a) has been normalized to the area in the energy range from 0.1 to -3.0 eV. The inset of Fig. 3(a) shows the temperature-dependent spectra of gold as a reference, which were well fitted to the Fermi-Dirac (FD) distribution function. Although the temperature-dependent spectra of gold show symmetric line shapes with the leading edge being midpoint exactly at E_F , asymmetric behavior is observed in the spectra of MnP. The unoccupied part in the spectra of MnP reveals strong temperature-dependent broadening, whereas there is much weaker temperature dependence from E_F to -100 meV. This can be explained by the pseudogap formation of ~ 100 meV size, which may be related to the ferromagnetic transition. Decreasing temperature induces spectral weight transfer from the peak at -100 meV in the paramagnetic state to the broad structure on the deeper side below -400 meV. The inset of Fig. 2 clearly reveals the spectral weight transfer depending on temperature. According to the band-structure calculation, the peak should be shifted with

temperature due to exchange splitting below T_C , whereas no significant shift of the -100 meV peak is observed. If the spectral weight below -400 meV is attributed to the exchange splitting of the d band, the present observation suggests that the exchange splitting in the material is independent of the temperature but that the spectral weight distribution is dependent on the temperature.

In order to clarify the temperature dependence of the spectral DOS near E_F , we have removed the effect of temperature broadening by dividing the spectra with the FD distribution function as shown in Fig. 3(b). The inset of Fig. 3(b) shows the spectra of gold, divided by the FD function, showing the flat DOS around E_F . Two kinds of temperature-dependent changes are observed. One is that the spectral weight of the broad maximum at -100 meV, appearing in the paramagnetic states, are transferred towards below -400 meV with decreasing temperature as shown in Fig. 2. The other is the “pseudogap” feature in the range from E_F to -100 meV, which develops at low temperatures. Spectral weight transfer gradually starts below T_C . The pseudogap formation near E_F starts below T_C and continues to develop even below T_N .

The temperature dependence of the pseudogap and the spectral weight transfer are summarized in Fig. 4. Here, the intensities at E_F , -100 meV and -800 meV below it are plotted. At E_F , spectral intensity shows a maximum at T_C . On the other hand, spectral intensity at -800 meV shows a minimum at T_C . Depression of the intensity at E_F with decreasing temperature may be related to the complex magnetic phase transition in MnP.

In conclusion, we have investigated the temperature-dependent electronic structure of MnP by high-resolution photoemission spectroscopy and the band-structure calculation. Photoemission spectra divided by Fermi-Dirac distribution function revealed two kinds of spectral changes depending on temperature, namely, the spectral weight transfer from -100 meV to -400 meV and the pseudogap formation of ~ 100 meV at E_F . Below T_C , a pseudogap was formed, which would relate to the ferromagnetic and helimagnetic phases.

One of the authors (J.O.) acknowledges support from the Japan Society for the Promotion of Science for Young Scientists.

*Present address: Department of Applied Chemistry, The University of Tokyo, Bunkyo-ku, Tokyo 113-8656, Japan.

¹MnP forms in the orthorhombic MnP-type structure (V_h^{16} , $Pbmn$ space group), which is distorted from the NiAs-type structure with $a=5.916$, $b=5.260$, and $c=3.173$ Å.

²T. Komatsubara, T. Suzuki, and E. Hirahara, J. Phys. Soc. Jpn. **28**, 317 (1970).

³E.E. Huber, Jr. and D.H. Ridgley, Phys. Rev. **135**, A1033 (1964).

⁴G.P. Felcher, J. Appl. Phys. **37**, 1056 (1966).

⁵C.C. Becerra, Y. Shapira, N.F. Oliveira, Jr., and T.S. Chang, Phys. Rev. Lett. **44**, 1692 (1980).

⁶C.C. Becerra, V. Bindilatti, and N.F. Oliveira, Jr., Phys. Rev. B **62**, 8965 (2000).

⁷A. Zieba, M. Slota, and M. Kucharczyk, Phys. Rev. B **61**, 3435 (2000).

⁸A. Kakizaki, H. Sugawara, I. Nagakura, and T. Ishii, J. Phys. Soc. Jpn. **49**, 2183 (1980); K. Naito, A. Kakizaki, T. Komatsubara, H. Sugawara, I. Nagakura, and T. Ishii, *ibid.* **54**, 416 (1985).

⁹A. Yanase and A. Hasegawa, J. Phys. C **13**, 1989 (1980).

¹⁰H. Yoshizawa, S.M. Shapiro, and T. Komatsubara, J. Phys. Soc. Jpn. **54**, 3084 (1985).

¹¹Y. Todate, K. Yamada, Y. Endoh, and Y. Ishikawa, J. Phys. Soc. Jpn. **56**, 36 (1987).

¹²H. Okuda, S. Senba, H. Sato, K. Shimada, H. Namatame, and M. Taniguchi, J. Electron Spectrosc. Relat. Phenom. **101-103**, 657 (1999).

¹³A. Continenza, S. Picozzi, W.T. Geng, and A.J. Freeman, Phys. Rev. B **64**, 085204 (2001).

¹⁴C. Kittel, Phys. Rev. **120**, 335 (1960).

¹⁵T. Okita and Y. Makino, J. Phys. Soc. Jpn. **25**, 120 (1968).

¹⁶A. Takase, H. Yashima, and T. Kasuya, J. Phys. Soc. Jpn. **47**, 531 (1979).

¹⁷A. Kakizaki, K. Ono, K. Tanaka, K. Shimada, and T. Sendohda, Phys. Rev. B **55**, 6678 (1997).

¹⁸Yu.S. Dedkov, U. Rudiger, and G. Guntherodt, Phys. Rev. B **65**, 064417 (2002).

¹⁹J.H. Park, E. Vescovo, H.J. Kim, C. Kwon, R. Ramesh, and T. Venkatesan, Nature (London) **392**, 794 (1998).

²⁰E. Kisker, K. Schroder, M. Campagna, and W. Gudat, Phys. Rev. Lett. **52**, 2285 (1984).

²¹J. Kanamori, *Core-level Spectroscopy in Condensed Systems*, edited by J. Kanamori and A. Kotani (Springer-Verlag, Berlin, 1988), p. 160.

²²T.J. Kreuzt, T. Greber, P. Aebi, and J. Osterwalder, Phys. Rev. B **58**, 1300 (1998).

²³T. Takahashi, Y. Naitoh, T. Sato, T. Kamiyama, K. Yamada, H. Hiraka, Y. Endoh, M. Usuda, and N. Hamada, Phys. Rev. B **63**, 094415 (2001).

²⁴T. Komatsubara, K. Kinoshita, and E. Hirakawa, J. Phys. Soc. Jpn. **20**, 2036 (1965).

²⁵M.C. Payne, M.P. Teter, D.C. Allan, T.A. Arias, and J.D. Johannopoulos, Rev. Mod. Phys. **64**, 1045 (1992); *CASTEP Users Guide* (Molecular Simulations Inc., San Diego, CA, 1998).

²⁶T. Suzuki, J. Phys. Soc. Jpn. **25**, 646 (1968).

²⁷J.-J. Yeh and I. Lindau, At. Data Nucl. Data Tables **32**, 1 (1985).